



Original Research

Magnetic Resonance Imaging Cerebrospinal Fluid Hydrodynamics in Patients with Meningitis

Devkant Lakhera¹, Rajiv Kumar Azad¹, Sheenam Azad², Ragini Singh³, Rohitash Sharma⁴

Departments of ¹Radiodiagnosis, ²Pathology, ³Pediatrics, and ⁴Neurology, Shri Guru Ram Rai Institute of Medical and Health Sciences, Dehradun, Uttarakhand, India.



***Corresponding author:**

Rajiv Kumar Azad,
Department of Radiodiagnosis,
Shri Guru Ram Rai Institute
of Medical and Health
Sciences, D6, Medical
Campus, Dehradun - 248 001,
Uttarakhand, India.

rajivas23@yahoo.com

Received : 25 February 2020

Accepted : 01 May 2020

Published : 19 May 2020

DOI

10.25259/JCIS_24_2020

Quick Response Code:



ABSTRACT

Objective: The objective of the study was to evaluate the cerebrospinal fluid (CSF) flow alterations in meningitis using phase-contrast magnetic resonance imaging (PCMRI).

Materials and Methods: Fifty patients with clinically confirmed or strongly suspected infectious meningitis and 20 controls were evaluated with MRI. Quantitative CSF analysis was performed at the level of cerebral aqueduct using cardiac-gated PCMRI. Velocity encoding (Venc) was kept at 20 cm/s. Patients were subdivided into Group I (patients with hydrocephalus [$n = 21$]) and Group II (patients without hydrocephalus [$n = 29$]).

Results: The mean peak velocity and stroke volume in controls were 2.49 ± 0.86 cm/s and 13.23 ± 6.84 μ l and in patients were 2.85 ± 2.90 cm/s and 16.30 ± 20.02 μ l, respectively. A wide variation of flow parameters was noted in meningitis irrespective of the degree of ventricular dilatation. A significant difference in peak velocity and stroke volume was noted in Group II as compared to controls. Viral meningitis showed milder alteration of CSF flow dynamics as compared to bacterial and tuberculous etiologies. At a cutoff value of 3.57 cm/s in peak CSF velocity, the specificity was 100% and sensitivity was 22.7% to differentiate between viral and non-viral meningitis.

Conclusion: Alteration of CSF flow dynamics on PCMRI can improve segregation of patients into viral and non-viral etiologies, especially in those in whom contrast is contraindicated or not recommended. This may aid in institution of appropriate clinical treatment.

Keywords: Meningitis, Cerebrospinal fluid, Phase-contrast Magnetic Resonance Imaging

INTRODUCTION

Meningitis is a life-threatening infectious disease that causes inflammation in the brain and spinal cord membranes. Rapid diagnosis is essential to improve prognosis.^[1,2] Neuroimaging has a crucial role in depiction of inflammatory changes in the brain and spine and may aid early diagnosis. It also helps in evaluation of subsequent complications and therapeutic response monitoring.^[3-5] Regardless of the advancements in magnetic resonance imaging (MRI), the optimal imaging protocol for diagnosing infectious meningitis remains contentious due to a lack of differentiation in enhancement in vessels and meninges on MRI and insufficient sensitivity in etiological characterization, primarily in the early stages. In addition, routine brain MRI imaging provides structural information but has a limited role in the assessment of CSF dynamics.^[6,7]

Phase-contrast MRI (PCMRI) with cardiac synchronism is a dynamic technique used to visualize cerebrospinal fluid (CSF) movement. This technique is non-invasive, highly sensitive even to slow

This is an open-access article distributed under the terms of the Creative Commons Attribution-Non Commercial-Share Alike 4.0 License, which allows others to remix, tweak, and build upon the work non-commercially, as long as the author is credited and the new creations are licensed under the identical terms.

©2020 Published by Scientific Scholar on behalf of Journal of Clinical Imaging Science

flow and provides precise and reproducible measurement of quantitative parameters.^[8] CSF flow may be altered in many intracranial and intraspinal pathologies. Over the past few decades, clinical research has demonstrated associations among changes in CSF hydrodynamics with meningitis, hydrocephalus, and cerebral edema.^[9-11]

There is a lack of sufficient literature on CSF dynamics in neuroinfectious conditions. In this study, we aimed to evaluate the pathophysiology of CSF flow alterations in meningitis and their related complications. Further, we investigated the utility of PCMRI as an alternate modality for identifying meningitis in patients in whom contrast is contraindicated and rapid diagnosis is required.

MATERIALS AND METHODS

The study was performed between 2016 and 2018 in a tertiary care hospital. It was a prospective case-control study comprising 50 patients with meningitis. The Institutional Ethical Committee approval was acquired and all eligible patients and guardians received a full explanation of the nature and purpose of the study. Written informed consent was obtained from all subjects. The study included patients with clinically confirmed or with a strong clinical suspicion of infectious meningitis. Those with a positive CSF culture were considered as clinically confirmed cases. Those with relevant clinical history, cytological findings in CSF, positive for biochemical markers (adenosine deaminase activity [ADA] and D-lactase), or positive for polymerase chain reaction on CSF and those exhibiting a therapeutic response were considered to have a strong suspicion of meningitis. Twenty subjects, undergoing MRI who had no significant imaging findings, formed the control group.

Data collection techniques and tools

Conventional MRI of the brain was performed before PCMRI using a 1.5 Tesla MR scanner (Magnetom, Siemens, Erlangen, Germany). Imaging parameters were axial spin-echo T1-weighted sequence (repetition time [TR] = 450–650 ms, echo time [TE] = 10–20 ms, section thickness = 5 mm, matrix = 256 × 192, number of excitations [NEX] = 2, field of view [FOV] = 230 cm, matrix size of 256 × 256); axial, coronal, and sagittal T2-weighted sequence (TR = 3000–4500 ms, TE = 80–90 ms, echo train length = 22–27, section thickness = 5 mm, matrix = 256 × 256, NEX = 2, FOV = 230 cm); and axial FLAIR sequence (TR = 7000–9000 ms, TE = 80–100 ms, inversion time = 2000–2300 ms, section thickness = 5 mm, matrix = 256 × 256, NEX = 1, FOV = 230 cm). Contrast-enhanced MRI was performed when indicated. After the administration of intravenous gadodiamide (Omniscan, GE Healthcare) at a dose of 0.1 mmol/kg body weight, a post-

contrast T1-weighted sequence with fat sat (TR = 556 ms, TE = 10 ms, echo train length = 58, matrix = 230 × 256) was acquired in all standard planes.

Phase-contrast imaging

For qualitative phase-contrast MRI, a two-dimensional fast low-angle shot (FLASH) sequence was used. T2-weighted sagittal images, phase, rephase, and magnitude images were obtained based on the following parameters: TR/TE = 34.45/9.73 ms; FOV = 240 mm; flip angle = 10°; and slice thickness = 4.5 mm. CSF flow dynamics were quantitatively studied using a prospective cardiac-gated high-resolution axial phase-contrast protocol (triggering performed using finger plethysmography) with an imaging plane perpendicular to the mid one-third of the cerebral aqueduct. The caudocranial direction was considered positive and the craniocaudal direction negative for directional programming in the software. The imaging parameters were TR/TE = 41.35/4.09 ms; FOV=320 mm; flip angle = 30°; and slice thickness = 5 mm. Velocity encoding (Venc) was kept at 20 cm/s. The total examination duration was approximately 15 min.

The acquired through-plane FLASH images were transferred to the post-processing Argus® software and CSF flow was qualitatively assessed at baseline after obtaining phase, rephase, and magnitude images in all subjects. The ROI was carefully manually drawn at the center of the aqueduct with size kept constant, i.e., 0.04 cm² to avoid systematic errors. The quantitative values were calculated by two radiologists who were blind to the subjects' clinical status and checked for consistency. The velocity was then plotted as a cardiac cycle function, allowing calculation of quantitative flow parameters. Changes in CSF flow were shown by automatic extraction of velocity time, peak velocity time, flow time, and net flow time graphics.

Statistical analysis

Data were analyzed using Microsoft Excel 2013 (Microsoft Corporation, NY, USA) and SPSS version 21 as mean (±SD), frequency, and percentage. Quantitative variables between the study groups were compared using an unpaired *t*-test for normal distribution or the Mann-Whitney U-test for non-normal distribution. The Chi-squared test was performed to compare categorical data. The expected frequency was <5 using Fisher's exact test. *P* < 0.05 was considered statistically significant. ROC curves were obtained by calculating the cutoff point of peak systolic velocity and stroke volume as tests for differentiating patients with viral from non-viral and tubercular from non-tubercular meningitis. The sensitivity, specificity, and accuracy were calculated from the ROC curves.

RESULTS

A total of 50 patients (22 females and 28 males) with the mean age of 20.93 ± 15.60 years (ranged 4 months–73 years) were enrolled in the study. The mean CSF peak velocity and stroke volume in controls were 2.49 ± 0.86 cm/s and 13.23 ± 6.84 μ l, respectively. No significant differences were noted in the CSF peak velocity or stroke volume between the age groups with no trend in flow parameters according to age. Qualitative analysis of cine MR images revealed normodynamic pulsatile flow through the cerebral aqueduct.

Out of the 50 included patients, 27 (54%) had associated complications such as hydrocephalus, vasculitis, and cerebral abscess. The most common complications were hydrocephalus (21 patients [42%]) and infarcts due to vasculitis (16 patients [32%]). Of the 50 patients with CSF-confirmed meningitis, 33 had tubercular, 6 had viral, 10 had pyogenic, and 1 had fungal meningitis. Subjects with tubercular meningitis had complications significantly higher than those with bacterial or viral meningitis.

The mean CSF peak velocity and stroke volume in patients were 2.85 ± 2.90 cm/s and 16.30 ± 20.02 μ l, respectively. The flow parameters did not significantly differ between patients and controls. However, the peak velocity and stroke volume were higher in patients than controls with a wide range in CSF flow parameters [Table 1].

Due to the wide variation in flow parameters with ventricular dilatation in the patients, this group was subdivided as follows:

Group I: Patients with hydrocephalus ($n = 21$).

Group II: Patients without hydrocephalus ($n = 29$).

In Group I, the mean peak velocity and stroke volume were 4.41 ± 3.90 cm/s and 16.30 ± 20.02 μ l, respectively. The flow parameters, particularly CSF peak velocity and stroke volume, were generally higher in these patients than controls [Table 2]. However, a lower peak systolic velocity of 1.41 cm/s was observed in 8 of the 21 patients. Reduced or absent CSF flow was detected at the aqueduct of Sylvius on cine images in these patients. Wide flow parameters variation was observed in Group I with peak velocities ranging from 0.813 to 16.59 cm/s and stroke volume ranging from 3.5 to 109 μ l with both hyper- and hypo-dynamic CSF circulation noted irrespective of the degree of ventricular dilatation. The cine MR images and quantitative parameters in a patient in Group I demonstrating hyperdynamic flow are shown in Figure 1.

Group II had mean CSF peak velocity and stroke volume of 1.71 ± 0.85 cm/s and 9.09 ± 6.91 μ l, respectively. The CSF flow parameters were lower in these patients as compared to controls, with CSF peak velocity ranging from 0.572 to 4.07 cm/s and stroke volume ranging from 1 to 23.5 μ l with

Table 1: Comparative values of quantitative cerebrospinal fluid flow parameters between patients ($n=50$) and controls ($n=20$).

Flow parameters	Patients	Control	P-value
Peak velocity (cm/s)	2.85±2.90	2.49±0.86	0.144
Average velocity (cm/s)	0.43±0.36	0.43±0.25	0.487
Average flow over range (ml/s)	0.02±0.04	0.02±0.03	0.214
Forward volume (μ l)	15.02±21.98	8.35±7.18	0.730
Reverse volume (μ l)	17.90±20.48	18.55±9.70	0.104
Net forward volume (μ l)	10.58±9.79	11.50±6.83	0.292
Stroke volume (μ l)	16.30±20.02	13.23±6.84	0.394

Table 2: Comparative values of quantitative cerebrospinal fluid flow parameters between patients (Group I) ($n=21$) and controls ($n=20$).

Flow parameters	Patients with hydrocephalus	Controls	P-value
Peak velocity (cm/s)	4.41±3.90	2.49±0.86	0.268
Average velocity (cm/s)	0.56±0.45	0.43±0.25	0.593
Average flow over range (ml/s)	0.03±0.06	0.02±0.03	0.906
Forward volume (μ l)	26.10±29.75	8.35±7.18	0.047*
Reverse volume (μ l)	26.91±27.77	18.55±9.70	0.896
Net forward volume (μ l)	14.10±12.75	11.50±6.83	0.814
Stroke volume (μ l)	26.26±27.13	13.23±6.84	0.235

*Significant

few patients showing near normal parameters. However, the difference in average values of these parameters in Group II and controls was statistically significant [Table 3]. On cine flow MR images, a larger group of patients exhibited reduced flow across the cerebral aqueduct. Reduced flow across the aqueduct in a patient in Group II is illustrated in Figure 2.

The average CSF flow parameters were higher in patients with tuberculous and bacterial meningitis than those with viral etiology. The peak systolic velocity and stroke volume in patients with bacterial, tubercular, and viral meningitis were 3.0 cm/s and 19.2 μ l, 3.01 cm/s and 16.8 μ l, and 1.87 cm/s and 10.8 μ l, respectively. Further, the range of parameters was wider in those with bacterial and tubercular meningitis with peak velocities of 0.9–16.59 cm/s and 0.57–11 cm/s, respectively, than in those with viral meningitis (1.23–3.53 cm/s).

The diagnostic accuracy of CSF peak velocity and stroke volume for the diagnosis of viral versus non-viral meningitis and tubercular versus non-tubercular was assessed by ROC curves. To differentiate between viral and non-viral meningitis, for CSF peak velocity, area under the receiver operator characteristic (ROC) curve (AUC) was 0.54 (95% CI – 0.35–0.72); at a cutoff value of 3.57 cm/s, the specificity

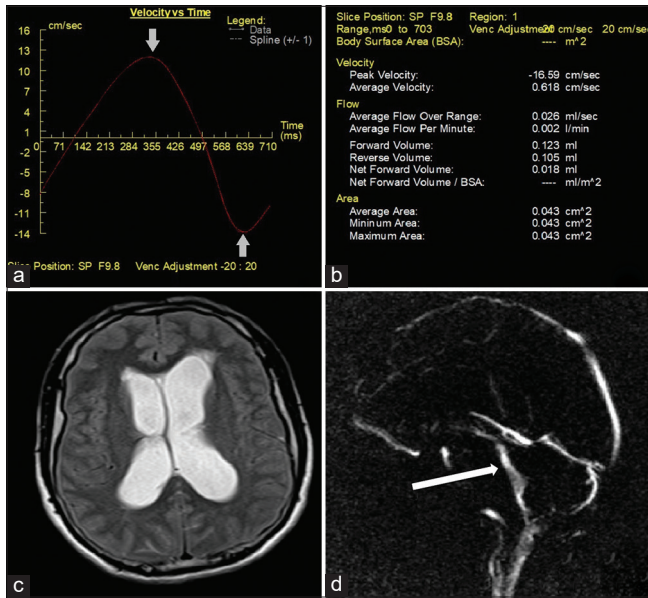


Figure 1: A 51-year-old male patient who presented with fever and headache diagnosed with meningitis. (a) Velocity time graphic on Argus post-processing showing normal pulsatile flow with elevated cerebrospinal fluid (CSF) peak velocity (arrows). (b) Quantitative CSF flow parameters. (c) magnetic resonance (MR) imaging Axial T2WI of brain showing hydrocephalus with mild periventricular ooze. (d) Magnitude cine MR image showing hyperdynamic flow across the cerebral aqueduct (arrow).

Table 3: Comparative values of quantitative cerebrospinal fluid flow parameters between patients (Group II) ($n=29$) and controls ($n=20$).

Flow parameters	Patients without hydrocephalus	Controls	P-value
Peak velocity (cm/s)	1.71±0.85	2.49±0.86	0.002*
Average velocity (cm/s)	0.34±0.25	0.43±0.25	0.132
Average flow over range (ml/s)	0.01±0.01	0.03±0.03	0.042*
Forward volume (μl)	7.00±7.41	8.35±7.18	0.313
Reverse volume (μl)	11.38±8.84	18.55±9.70	0.008*
Net forward volume (μl)	8.03±5.97	11.50±6.83	0.067
Stroke volume (μl)	9.09±6.91	13.23±6.84	0.024*

*Significant

was 100% and sensitivity was 22.7%; while for stroke volume, AUC was 0.56 (95% CI – 0.35–0.78); at a cutoff values of 6.75 μl, the specificity was 66.7% and sensitivity was 63.6%. In differentiation between tubercular and non-tubercular meningitis, for CSF peak velocity, AUC was 0.61 (95% CI – 0.44–0.77); at a cutoff value of 2.58 cm/s, the specificity was 88.2% and sensitivity was 45.5%; while for stroke volume, AUC was 0.59 (95% CI – 0.42–0.76); at a cutoff values of

4.75 μl, the specificity was 35.3% and sensitivity was 84.8%. The same is illustrated in Figure 3.

DISCUSSION

Neurological infections account for a substantial burden of disease and are a cause for great concern in developing countries.^[12] Early diagnosis and etiological segregation based on imaging features is of crucial clinical importance and can allow for the initiation of appropriate therapy and prevention of complications.^[13,14] Our understanding of CSF hydrodynamics on MRI in such patients is limited, with most studies performed on patients with ventriculomegaly.^[15,16]

Significant emphasis has been placed on the evaluation of CSF flow through the cerebral aqueduct and CSF peak velocities in healthy volunteers.^[17] The previous studies have identified a large variation in physiological range of CSF flow quantification with peak velocities of 1.41–11.67 cm/s. The average CSF flow parameters in controls in the present study were closer to the flow values noted in the study done by Nitz *et al.* who used a similar scanner.^[18]

Our findings indicated a wide variation in flow parameters in Group I (patients with hydrocephalus) with peak velocities and stroke volumes of 0.813–16.59 cm/s and 3.5–109 μl, respectively, suggesting the existence of different pathogenetic mechanisms altering the CSF flow. A plausible explanation is the complex type hydrocephalus observed in meningitis, wherein both absorption and flow may be interrupted, leading to both communicating and non-communicating types of hydrocephalus. In both the cases, the likely cause is exudates in subarachnoid spaces or ventricular system as a result of inflammation. In the early phases of meningitis, the accumulation of exudates in the subarachnoid spaces, particularly along the brain base (i.e., the interpeduncular and ambient cisterns), may cause communicating hydrocephalus. In the subset of patients with reduced flow parameters, subarachnoid or intraventricular inflammation is a likely cause of aqueductal obstruction. This was evidenced by the reduced aqueductal flow on cine MR images and consistent with the studies by Lucic *et al.*, Parkkola *et al.*, and Abdelhameed *et al.*, wherein reduced aqueductal flow was observed in patients with hydrocephalus as a result of aqueductal stenosis.^[19-21] This further affirms the role of PCMRI in the differentiation of communicating and non-communicating hydrocephalus.

Surprisingly, we observed significantly lower flow parameters in Group II (meningitis without hydrocephalus), wherein the CSF peak velocity and stroke volume were 1.71 ± 0.85 cm/s and 9.09 ± 6.91 μl. On cine flow MR images, a larger group of patients exhibited reduced flow across the cerebral aqueduct. To the best of our knowledge, there have been no prior PCMRI studies for CSF dynamics in such a group of patients.

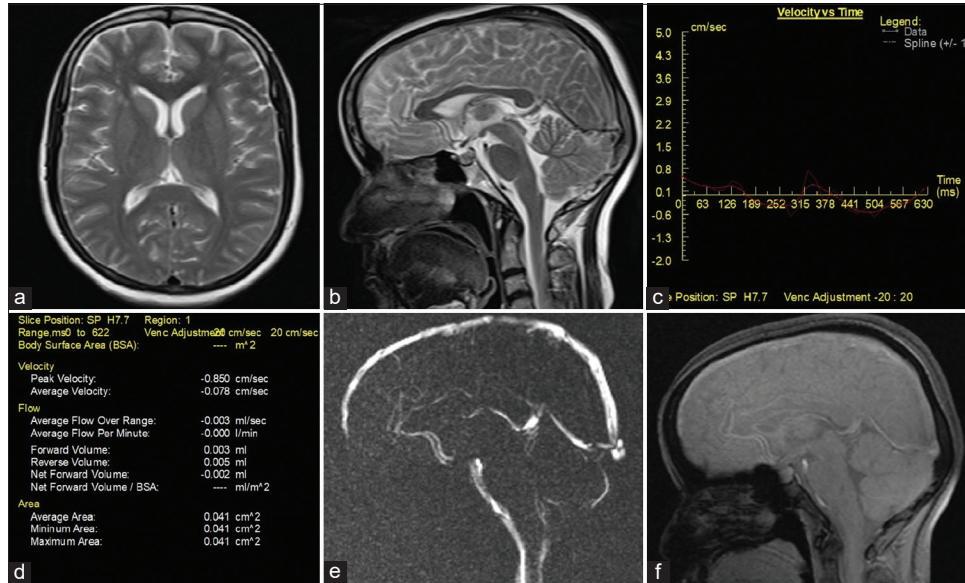


Figure 2: A 26-year-old female patient who presented with fever and neck rigidity diagnosed with meningitis. (a and b) Axial and sagittal magnetic resonance (MR) imaging T2WI of brain show absence of hydrocephalus. (c) Velocity time graphic showing irregular non pulsatile flow across aqueduct. (d) Reduced quantitative flow parameters. (e and f) Cine MR magnitude and phase images showing reduced flow at the level of cerebral aqueduct.

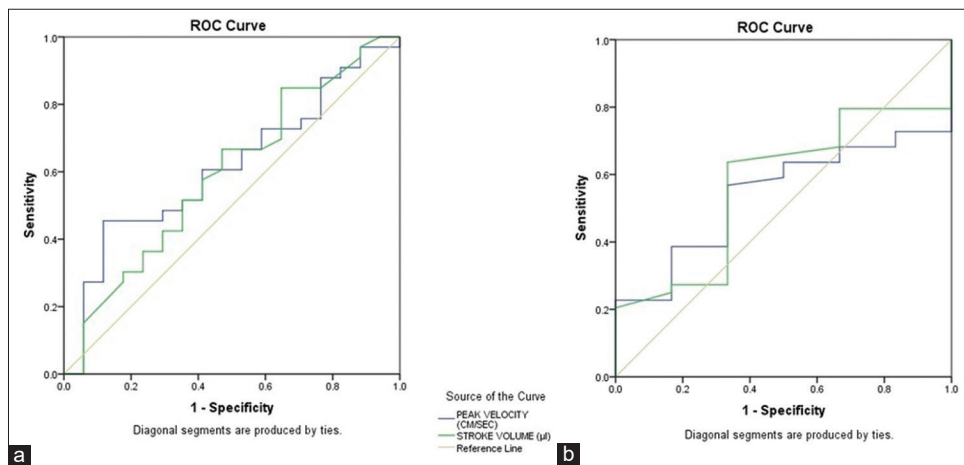


Figure 3: Receiver operator characteristic curves for comparison of cerebrospinal fluid peak velocity and stroke volume for etiological differentiation of patients with meningitis. (a) Tubercular versus non-tubercular meningitis. (b) Viral versus non-viral meningitis.

A reduction in aqueductal flow could possibly be attributed to changes in CSF concentrations of inflammatory infiltrates/exudates in the early phase of meningitis. Inflammatory damage to the blood-CSF barrier increases the permeability to CSF proteins, leading to elevated levels in the CSF, which may alter viscosity and flow dynamics. This could explain the shorter irregular and non-pulsatile temporal CSF flow waveform on flow versus time graphs. Subsequently, in later stages, as inflammation increases, CSF absorption is curtailed by obstruction in arachnoid villi with further elevations in intracranial pressure and neurological sequelae such as hydrocephalus, leading to hyperdynamic flow patterns.

The pathological elevation of protein levels in the CSF that is observed in neurological diseases has been explained quantitatively by changes in the CSF flux rate, due to reduced volume exchange, or an increase in the molecular net flux into CSF without a change in permeability coefficients. However, the physiology of flow cannot be accurately accounted for by the fundamental principles of fluid biomechanics due to the structural complexity of the brain and subarachnoid spaces.^[22]

Increase in CSF protein concentrations has also been reported in different etiologies such as reduced CSF flow through the arachnoid villi in inflammatory diseases or

conditions causing a blockade of the subarachnoid space. Experimental studies by Scheld *et al.* and Fuhrmeister *et al.* have demonstrated marked alterations in CSF hydrodynamics in the acute stage of meningitis with elevation in CSF pressure and outflow resistance. However, their studies also suggested a 5–10-fold reduction in the CSF formation rate at basal intracranial pressure in the presence of meningitis.^[10,11]

We found that patients with tuberculous and bacterial meningitis showed higher average CSF flow parameters as compared to those with viral etiology possibly indicating higher propensity to alter the CSF flow dynamics. In these etiologies, the bacteria have a higher tendency to disrupt the blood–brain barrier, causing the inflammatory cells and proteins to leak into the subarachnoid space and form exudates.^[23,24] This was supported by the cytochemical CSF analyses in these patients, which revealed significant CSF leukocytosis, CSF-ADA, and higher CSF protein concentrations (>50 mg/dl) attributed to the substantially wider CSF flow alterations. Conversely, in viral meningitis, milder dysfunction of blood brain barrier is observed with unremarkable CSF laboratory parameters accounting for lower alteration in CSF flow. CSF peak velocity showed a high specificity (i.e., 100%) with a cutoff of 3.57 cm/s in differentiation of viral versus non-viral meningitis as assessed by ROC curves which was higher compared to stroke volume. This could be of value in differentiation between viral and non-viral causes meningitis.

Bacterial and viral meningitis can be largely indistinguishable, especially in early stages. Obtaining CSF for laboratory examination is an invasive, technically difficult, and time-consuming procedure, and CSF parameters may be unequivocal with several studies reporting high false-negative lumbar puncture rates. This leads to an uncertainty in management protocol and thus an empirical antimicrobial therapy along with adjunctive dexamethasone is administered which may be potentially harmful to the patient. A cutoff value of CSF peak velocity to suggest a non-viral cause can aid in formulation of an individualized treatment protocol with reduced administration of antibiotics in such patients where it may be harmful. Further, PCMRI is non-invasive and is performed without the requirement of intravenous contrast agents. This can be particularly useful in pediatric patients and those with a history of contrast allergy or renal failure.

A technical limitation in our study was related to the placement of the ROI due to small size of the aqueduct which may be a source of variability between measurements, affecting the mean systolic velocity.^[25] Another limitation was prospective gating used in our study to reduce the time of scan, which may produce less accurate quantitative results as compared to retrospective gating.

CONCLUSION

Altered CSF flow dynamics were observed in meningitis patients, with both hyper- and hypo-dynamic flow, particularly in the presence of hydrocephalus. PCMR may be effective in conjunction with conventional MRI in the assessment and differentiation of communicating and non-communicating hydrocephalus. The significantly reduced parameters in patients without hydrocephalus could potentially have an affirmative role in the early diagnosis of meningitis. Alterations in CSF flow dynamics, along with clinical and radiological features, may aid in segregation into viral and non-viral causes of meningitis and assist in instillation of appropriate treatment. This is especially true in pediatric patients and those in whom intravenous contrast is not approved for imaging. However, further studies with stronger magnets are required to substantiate our findings. Evaluation of arterial and venous flow can provide further insight into changes in intracranial flow dynamics in meningitis. Technical improvements in the measurement of CSF flow may improve our understanding of CSF flow hydrodynamics and lead to better utilization of this technique in the clinical setting.

Declaration of patient consent

The Institutional Review Board (IRB) permission obtained for the study.

Financial support and sponsorship

Nil.

Conflicts of interest

There are no conflicts of interest.

REFERENCES

- Scheld WM, Koedel U, Nathan B, Pfister HW. Pathophysiology of bacterial meningitis: Mechanism(s) of neuronal injury. *J Infect Dis* 2002;186:S225-33.
- Hoffman O, Weber RJ. Pathophysiology and treatment of bacterial meningitis. *Ther Adv Neurol Disord* 2009;2:1-7.
- Chang KH, Han MH, Roh JK, Kim IO, Han MC, Kim CW. Gd-DTPA-enhanced MR imaging of the brain in patients with meningitis: Comparison with CT. *AJNR Am J Roentgenol* 1990;11:69-76.
- Hughes DC, Raghavan A, Mordekar SR, Griffiths PD, Connolly DJ. Role of imaging in the diagnosis of acute bacterial meningitis and its complications. *Postgrad Med J* 2010;86:478-85.
- Splendiani A, Puglielli E, De Amicis R, Necozone S, Masciocchi C, Gallucci M. Contrast-enhanced FLAIR in the early diagnosis of infectious meningitis. *Neuroradiology* 2005;47:591-8.

6. Mathews VP, Kuharik MA, Edwards MK, D'Amour PG, Azzarelli B, Dreesen RG. Dyke award. Gd-DTPA-enhanced MR imaging of experimental bacterial meningitis: Evaluation and comparison with CT. *AJR Am J Roentgenol* 1989;152:131-6.
7. Meltzer CC, Fukui MB, Kanal E, Smirniotopoulos JG. MR imaging of the meninges. Part I. Normal anatomic features and nonneoplastic disease. *Radiology* 1996;201:297-308.
8. Yamada S, Tsuchiya K, Bradley WG, Law M, Winkler ML, Borzage MT, *et al.* Current and emerging MR imaging techniques for the diagnosis and management of CSF flow disorders: A review of phase-contrast and time-spatial labeling inversion pulse. *AJNR Am J Neuroradiol* 2015;36:623-30.
9. Negahdar MJ, Shakeri M, McDowell E, Wells J, Vitaz T, Harkema S, *et al.* Cine Phase-Contrast MRI Measurement of CSF Flow in the Cervical Spine: A Pilot Study in Patients with Spinal Cord Injury. Florida, United States: Proceeding SPIE 7965, Medical Imaging 2011: Biomedical Applications in Molecular, Structural, and Functional Imaging; 2011.
10. Fuhrmeister U, Ruether P, Dommasch D, Gaab M. Alterations of CSF hydrodynamics following meningitis and subarachnoid hemorrhage. In: Shulman K, Marmarou A, Miller JD, Becker DP, Hochwald GM, Brock M, editors. *Intracranial Pressure IV*. Berlin: Springer; 1980. p. 241-3.
11. Scheld WM, Dacey RG, Winn HR, Welsh JE, Jane JA, Sande MA. Cerebrospinal fluid outflow resistance in rabbits with experimental meningitis. Alterations with penicillin and methylprednisolone. *J Clin Invest* 1980;66:243-53.
12. Jayaraman Y, Veeraraghavan B, Purushothaman GK, Sukumar B, Kangusamy B, Kapoor AN, *et al.* Burden of bacterial meningitis in India: Preliminary data from a hospital based sentinel surveillance network. *PLoS One* 2018;13:e0197198.
13. McIntyre PB, O'Brien KL, Greenwood B, Van De Beek D. Effect of vaccines on bacterial meningitis worldwide. *Lancet* 2012;380:1703-11.
14. Edmond K, Clark A, Korczak VS, Sanderson C, Griffiths UK, Rudan I. Global and regional risk of disabling sequelae from bacterial meningitis: A systematic review and meta-analysis. *Lancet Infect Dis* 2010;10:317-28.
15. Bradley WG Jr., Kortman KE, Burgoyne B. Flowing cerebrospinal fluid in normal and hydrocephalic states: Appearance on MR images. *Radiology* 1986;159:611-6.
16. Kartal MG, Algin O. Evaluation of hydrocephalus and other cerebrospinal fluid disorders with MRI: An update. *Insights Imaging* 2014;5:531-41.
17. Unal O, Kartum A, Avcu S, Etlik O, Arslan H, Bora A. Cine phase-contrast MRI evaluation of normal aqueductal cerebrospinal fluid flow according to sex and age. *Diagn Interv Radiol* 2009;15:227-31.
18. Nitz WR, Bradley WG Jr., Watanabe AS, Lee RR, Burgoyne B, O'Sullivan RM, *et al.* Flow dynamics of cerebrospinal fluid: Assessment with phase-contrast velocity MR imaging performed with retrospective cardiac gating. *Radiology* 1992;183:395-405.
19. Lucic MA, Koprivsek K, Kozic D, Spero M, Spirovski M, Lucic S. Dynamic magnetic resonance imaging of endoscopic third ventriculostomy patency with differently acquired fast imaging with steady-state precession sequences. *Bosn J Basic Med Sci* 2014;14:165-70.
20. Abdelhameed AM, Darweesh EA, Bedair MH. Role of MRI CSF flowmetry in evaluation of hydrocephalus in pediatric patients. *Egypt J Hosp Med* 2017;68:1291-6.
21. Parkkola RK, Komu ME, Aärimaa TM, Alanen MS, Thomsen C. Cerebrospinal fluid flow in children with normal and dilated ventricles studied by MR imaging. *Acta Radiol* 2001;42:33-8.
22. Reiber H. Flow rate of cerebrospinal fluid (CSF)--a concept common to normal blood-CSF barrier function and to dysfunction in neurological diseases. *J Neurol Sci* 1994;122:189-203.
23. Sharma D, Shah I, Patel S. Late onset hydrocephalus in children with tuberculous meningitis. *J Fam Med Prim Care* 2016;5:873-4.
24. Chander A, Shrestha CD. Cerebrospinal fluid adenosine deaminase levels as a diagnostic marker in tuberculous meningitis in adult Nepalese patients. *Asian Pac J Trop Dis* 2013;3:16-9.
25. Korbecki A, Zimny A, Podgórski P, Szaśiadek M, Bładowska J. Imaging of cerebrospinal fluid flow: Fundamentals, techniques, and clinical applications of phase-contrast magnetic resonance imaging. *Pol J Radiol* 2019;84:240-50.

How to cite this article: Lakhera D, Azad RK, Azad S, Singh R, Sharma R. Magnetic Resonance Imaging Cerebrospinal Fluid Hydrodynamics in Patients with Meningitis. *J Clin Imaging Sci* 2020;10:29.